J Solid State Electrochem (2004) 8: 923–927
DOI 10.1007/s10008-004-0510-4

ORIGINAL PAPER

Sven Uhlenbruck · Frank Tietz · Vincent Haanappel
Doris Sebold · Hans-Peter Buchkremer · Detlev Stöver

Silver incorporation into cathodes for solid oxide fuel cells operating at intermediate temperature

Received: 6 October 2003 / Accepted: 6 January 2004 / Published online: 23 March 2004

Abstract Silver (Ag) at 0.1–2.0 wt% was incorporated into cathodes for solid oxide fuel cells as a catalyst for oxygen reduction. A novel processing route for Ag incorporation ensuring a very homogeneous Ag ion distribution is presented. From the results of X-ray powder diffraction it can be concluded that the $La_{0.65}Sr_{0.3}MnO_{3-\delta}$ perovskite phase is already formed at 900 °C. The solubility of Ag in the crystal lattice in this type of perovskite was below 1 wt%. The electrochemical tests of these materials show that there is only a slight catalytic effect of Ag. Scanning electron microscopy reveals a low mechanical contact of the cathode grains to the electrolyte due to the low cathode sintering temperature that was chosen.

Keywords Solid oxide fuel cell · Cathode · Silver

Introduction

Fuel cells can convert chemical energy into electricity without the intermediate step of heat generation. Therefore the efficiency of such a device is not limited by the Carnot efficiency of heat engines. The development of the well-known polymer electrolyte (or proton exchange) membrane (PEM) fuel cells suffers from the high cost of platinum catalysts and the need to be operated with high-purity hydrogen without carbon monoxide (catalyst poisoning). Solid oxide fuels cells (SOFCs) overcome these problems as they are operated at 800–1,000 °C where the electrode materials have sufficient catalytic activity and carbon monoxide in the fuel gas can be easily oxidized and desorbed. The SOFC can even be powered with hydrocarbons. Nevertheless, the high operating temperature causes problems, too. High temperature leads to enhanced aging and requires heat-resistant system components (e.g. interconnect plates for connecting single fuel cells; heat exchangers). Lowering the temperature, however, decreases the power density of SOFCs due to the decreasing catalytic activity.

Silver (Ag) is known to improve the oxygen exchange reaction activity [1, 2]. Therefore, attempts were made to mix or to impregnate SOFC cathodes (e.g. $La_xSr_y MnO_{3-\delta}$) with Ag [3, 4]. Problems can arise during impregnation due to low adhesion forces between the Ag precursor solutions and the ceramic cathode material. On the other hand, mechanical mixing of metals and ceramics always suffers from the ductility of the metal. Metal particles cannot be milled to the desired particle size, and if milled the particles are rolled to irregular flat bands which would destroy the microstructure of the cathode. Using Ag salts instead of solid Ag metal has proved to be detrimental to the power density of fuel cells with such cathodes [4].

In this paper an alternative method for incorporating Ag into ceramic cathodes is presented that is suitable for producing a very homogeneous distribution of Ag on an atomic scale. These cathode materials were characterized by X-ray powder diffraction (XRD), surface area [according to Brunauer, Emmett and Teller (BET)] and scanning electron microscopy (SEM). The influence of Ag on the electrochemical performance of the cathode material was evaluated by single fuel cell tests.

Materials and methods

The ceramic cathode material with the nominal composition $La_{0.65}Sr_{0.3}MnO_{3-\delta}$ along with Ag was prepared by a citrate complexation method (Pechini method) [5]: nitrate salts of La, Sr, Mn and Ag (Merck, Germany, quality: analytical pure) were dissolved in de-ionized water and stirred well. This method has the advantage that, in contrast to earlier experiments using oxides, carbonates, hydroxides and nitrates simultaneously [1, 2], the solution con-

S. Uhlenbruck (✉) · F. Tietz · V. Haanappel · D. Sebold
H.-P. Buchkremer · D. Stöver
Forschungszentrum Jülich GmbH, Institute for Materials and Processes in Energy Systems, IWV, 52425 Jülich, Germany
E-mail: s.uhlenbruck@fz-juelich.de
Tel.: +49-2461-616858
Fax: +49-2461-612455

tained—besides the water as the solvent—solely the desired cations and $(NO_3)^-$ ions. Thus, no reaction between the set of cations and different types of anions can take place, e.g. the cations Ag^+ and Mn^{2+} may react with $(CO_3)^{2-}$ ions and precipitate as Ag_2CO_3 and $(MnCO_3)$, which are almost insoluble in water.

An excess of citric acid (>2 moles per mole cation) was added to this solution in order to obtain a complexation of the cations. Ethylene glycol was added in excess (>5 moles per mole citric acid) to polymerize the solution. The temperature of this gel was gently increased to 700 °C to combust all organic compounds and to decompose the $(NO_3)^-$ ions. The residue was a fine dark black powder.

The pure $La_{0.65}Sr_{0.3}MnO_{3-\delta}$ without Ag which was used as a reference was a spray-pyrolyzed powder (for details see [6]).

Chemical analysis was performed using an inductively coupled plasma optical emission spectroscope (ICP-OES), XRD using a Siemens D 500 X-ray diffractometer and surface area determination by means of BET Areameter II (Ströhlein). SEM imaging was carried out with a LEO 1530 electron microscope.

In order to obtain fuel cells with these Ag-containing cathodes the synthesized powders were first mixed with terpineol and ethyl cellulose to a paste and then screen-printed on top of an 8 mol% yttria-stabilized zirconia (8YSZ) electrolyte of about 5 μm in thickness that was mechanically supported by a NiO/8YSZ anode substrate of 1.5 mm in thickness. Details of the processing of the anode and the electrolyte can be found in [7, 8, 9]. The sintering of the cathode was carried out at 920 °C for 3 h in air. A significant increase in sintering temperature of the Ag-containing cathode materials was avoided due to the low melting point of Ag (961 °C).

The screen printing of the cathode was carried out in two steps: firstly, a "functional layer" of 15 μm in thickness consisting of a mixture of 8YSZ and $La_{0.65}Sr_{0.3}MnO_{3-\delta}$ (+Ag), and secondly, a 30 μm thick layer of pure $La_{0.65}Sr_{0.3}MnO_3$. The introduction of such a functional layer has three advantages: this layer reduces the mismatch in the thermal expansion coefficient between $La_{0.65}Sr_{0.3}MnO_{3-\delta}$ (12.5×10^{-6} 1/K) and 8YSZ (10.5×10^{-6} 1/K); the three-phase boundary of the electrode/electrolyte/gas where the reduction of oxygen takes place is increased so that the effective electrochemical active area is enhanced and more oxygen ions per time period are fed to the electrolyte; and the grain growth of $La_{0.65}Sr_{0.3}MnO_{3-\delta}$ during sintering and operation is (at least partially) suppressed and thus the surface area where oxygen can react is not decreased.

The electrochemical cell tests were performed in an alumina housing using gold seals, air on the cathode side (1,000 ml min^{-1}) and hydrogen (1,000 ml min^{-1}) containing 3 vol.% water vapor on the anode side. The electrical contact was made by means of a fine platinum mesh on the air side of the fuel cell and a nickel mesh on the fuel side [10].

Results and discussion

Table 1 shows the results of the chemical analysis and the BET surface area for the Ag-containing $La_{0.65}Sr_{0.3}MnO_{3-\delta}$ cathode materials calcined at 900 °C and for the Ag-free $La_{0.65}Sr_{0.3}MnO_{3-\delta}$. Within the accuracy of ICP-OES (±3%) the measured compositions agree well with the nominal stoichiometry. Therefore, the nominal composition is hereafter used to denote the ceramic material.

The BET surface area was around 5 m^2/g for all samples, which is in the same range as for the Ag-free powder (4.7 ± 0.5 m^2/g), so no influence of Ag on the BET surface area was found.

With respect to the XRD patterns (Fig. 1) it can be concluded that the material crystallized in a perovskite structure irrespective of the addition of Ag. From these data no significant shifts of the peak positions (and thus no significant variations in the lattice parameters) due to a possible incorporation of Ag as Ag^+ ions on the A-site position of an ABO_3 perovskite (as stated for $La_{0.7}Ag_{0.3}Fe_{0.5}Co_{0.5}O_3$ in [2]) into the lattice could be detected.

Figure 2 shows the XRD pattern for $La_{0.65}Sr_{0.3}MnO_{3-\delta}$ with 1 wt% Ag on an enlarged scale. Traces of $La(OH)_3$ and Mn_3O_4 (which appear in the other specimens, too) are visible. In our experience such small traces have no detrimental influence on the performance of $La_{0.65}Sr_{0.3}MnO_{3-\delta}$ cathodes in SOFCs.

Moreover, a peak that corresponds to solid Ag metal is found (referring to JCPDS No. 4–0783). That means that the solubility limit for Ag in this type of perovskite seems to be significantly lower than about 1 wt% Ag—a fact that was not observed previously [2]. At lower Ag concentrations, Ag peaks could not be detected in the diffraction patterns because of the detection limit of XRD for proportions lower than about 1 vol.%. Even at 1 wt% and 2 wt% it is difficult to identify the solid Ag metal since the relative intensity of the Ag diffraction pattern is low and the Ag peaks are rather close to the perovskite and $La(OH)_3$ and Mn_3O_4 peaks. Nevertheless, these peaks could not be accounted for by either the $La(OH)_3$, Mn_3O_4 or the perovskite peaks.

In Fig. 3 and Fig. 4 the results of the electrochemical cell tests are presented. At 800 °C the current densities are in the range of 0.5–0.6 A/cm^2 for a cell voltage of 0.7 V. They are comparable to values for a Ag-free reference cell that was sintered at 920 °C (0.49 ± 0.03 A/cm^2 at 0.7 V; averaged values based on tests of two cells). Therefore, no significant improvement due to Ag doping is found. This is apparently different when the temperature is lowered to 750 °C. The averaged current density for the cell with the undoped cathode is 0.28 ± 0.02 A/cm^2, while it is 0.38 ± 0.05 A/cm^2 for the Ag-containing samples. Nonetheless, in the range of 0.1–2 wt% Ag, no influence of the amount of Ag on the power density could be detected (Fig. 4).

Table 1 Chemical analysis of the synthesized ceramic powders calcined at 900 °C for 5 h

Nominal	Measured[a]	BET surface (m^2/g)
$La_{0.65}Sr_{0.3}MnO_{3-\delta}$ + 0.1 wt% Ag	$La_{0.66}Sr_{0.30}MnO_{3-\delta}$ + 0.11 wt% Ag	4.3 ± 0.4
$La_{0.65}Sr_{0.3}MnO_{3-\delta}$ + 0.5 wt% Ag	$La_{0.66}Sr_{0.30}MnO_{3-\delta}$ + 0.50 wt% Ag	4.5 ± 0.5
$La_{0.65}Sr_{0.3}MnO_{3-\delta}$ + 1.0 wt% Ag	$La_{0.66}Sr_{0.30}MnO_{3-\delta}$ + 0.92 wt% Ag	5.3 ± 0.5
$La_{0.65}Sr_{0.3}MnO_{3-\delta}$ + 2.0 wt% Ag	$La_{0.66}Sr_{0.30}MnO_{3-\delta}$ + 1.96 wt% Ag	5.1 ± 0.5
$La_{0.65}Sr_{0.3}MnO_{3-\delta}$	$La_{0.66}Sr_{0.31}MnO_{3-\delta}$	4.7 ± 0.5

[a]Mn fraction set to 1 by definition

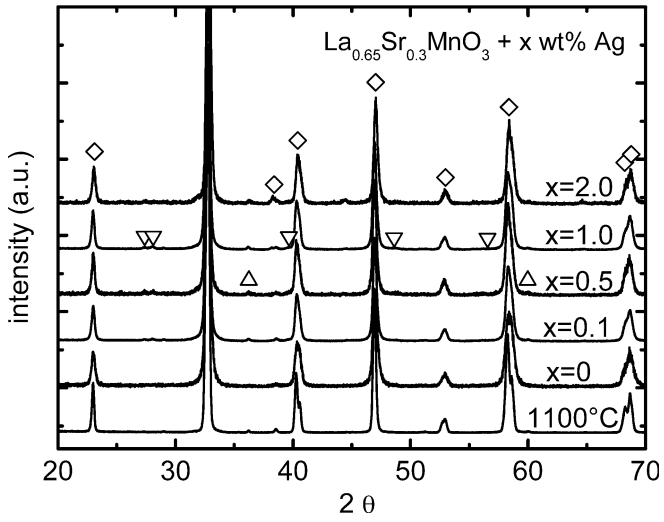

Fig. 1 X-ray diffraction patterns of $La_{0.65}Sr_{0.3}MnO_{3-\delta}$ with 0–2 wt% silver (Ag) sintered at 900 °C for 5 h. The *diamonds* show the position of the perovskite peaks referring to phase-pure $La_{0.65}Sr_{0.3}MnO_{3-\delta}$ (related to JCPDS No. 32–0484). *Triangles* pointing *downwards* and *upwards* denote peak positions that correspond to $La(OH)_3$ (JCPDS No. 6–0585) and Mn_3O_4 (JCPDS No. 27–0734), respectively. The X-ray powder diffraction pattern labeled "*1,100* °C" corresponds to $La_{0.65}Sr_{0.3}MnO_{3-\delta}$ sintered at 1,100 °C

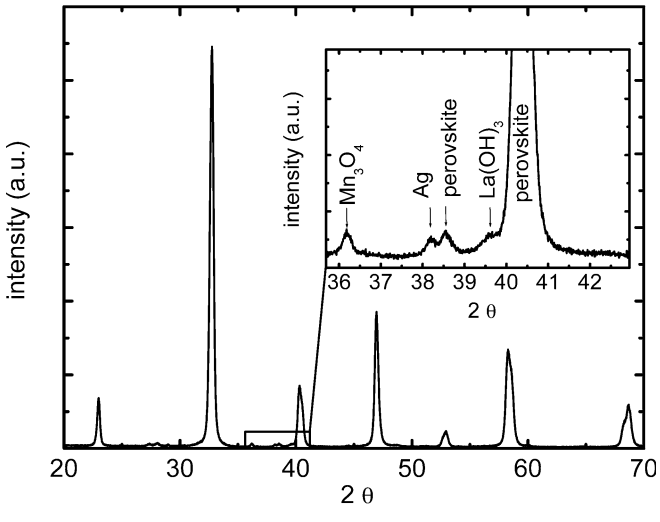

Fig. 2 $La_{0.65}Sr_{0.3}MnO_{3-\delta}$ with 1 wt% Ag, calcined at 900 °C for 5 h. In the *inset* one of the Ag peaks is visible, and the proportion of secondary phases ($La(OH)_3$ and Mn_3O_4) can be estimated

The linear range of the slope of the current density-voltage curves in Fig. 3 describes the area-specific "internal" resistance of the fuel cells. The internal resistances as a function of temperature approximately follow a simple Arrhenius activation law [$\propto \exp(E/kT)$, where E is apparent activation energy, k is theBoltzmann's constant, and T the absolute temperature). The apparent activation energies (including errors) of the investigated cells were calculated using a least squares fit routine applied to the respective Arrhenius plots. For each calculation, data points of at least four temperatures were taken into account (650–800 °C for Ag-containing cells, 750–900 °C for Ag-free cells). These activation energies are shown in Fig. 5. Compared to the results for the undoped specimen sintered at 920 °C, the resulting data for the apparent activation energies suggest that they are slightly reduced due to Ag incorporation, and thus there is a small electrocatalytic effect.

The Ag metal seemed to be homogeneously distributed. However, it was not possible to visualize Ag solid metal segregations in the cathodes by SEM. Firstly, the

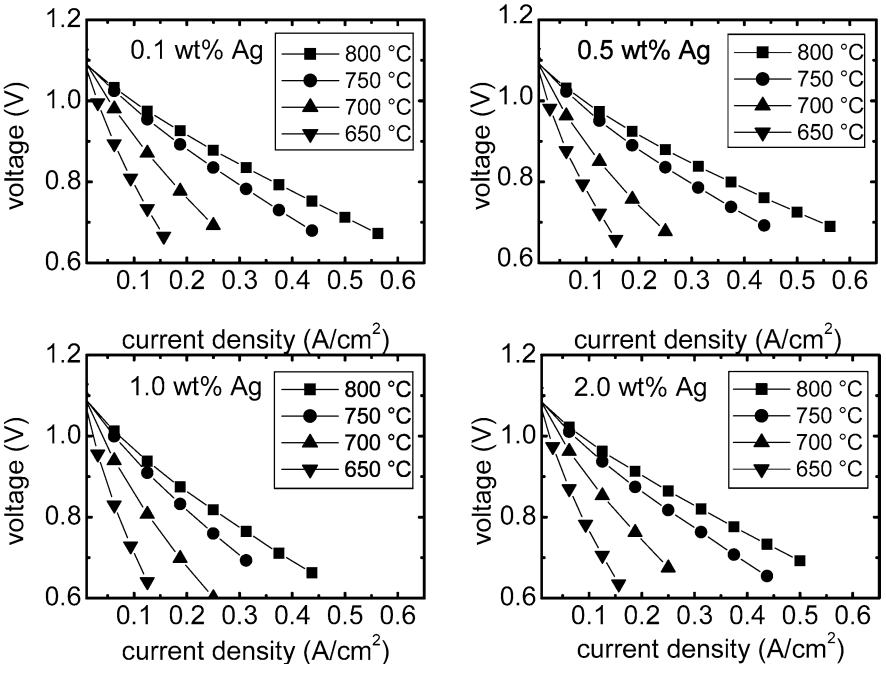

Fig. 3 Current voltage curves of cells with Ag-doped $La_{0.65}Sr_{0.3}MnO_{3-\delta}$ cathodes

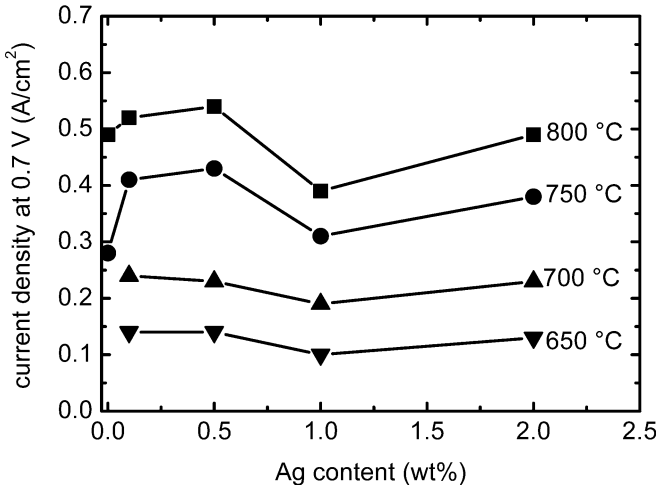

Fig. 4 Current densities of Ag-containing $La_{0.65}Sr_{0.3}MnO_{3-\delta}$ cathodes, sintered at 920 °C, vs. Ag content in the cathode

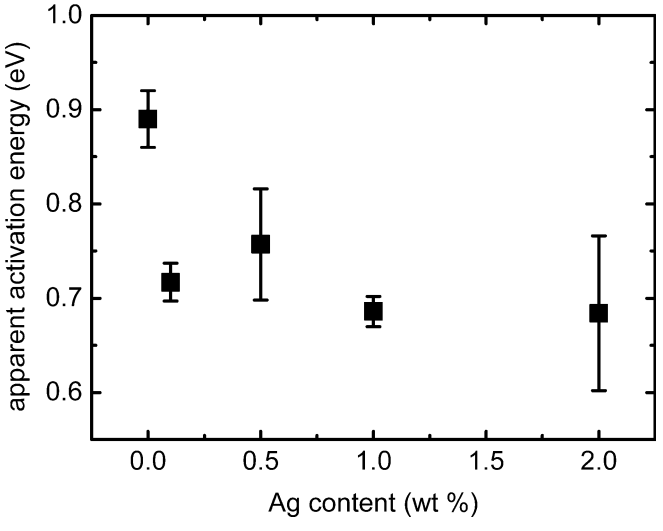

Fig. 5 Apparent activation energies extracted from the Arrhenius-like thermally activated internal resistances. The smaller the *error bars* the better the data points in the Arrhenius plots fit to a linear curve

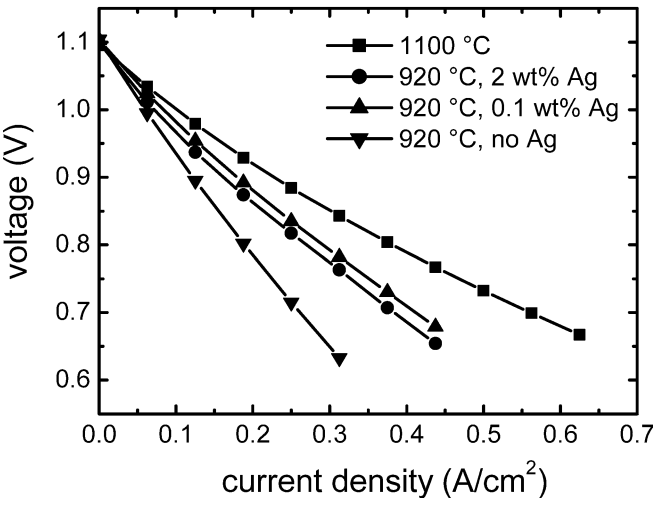

Fig. 6 Current-voltage curves of cells with cathodes without Ag, sintered at 1,100 °C (*squares*), and of cells with cathodes with 0.1 wt% (*triangles pointing upwards*), 2 wt% Ag (circles) and no addition of Ag (*triangles pointing downwards*), sintered at 920 °C

fracture surfaces of the cells were analyzed in "secondary electron mode" for optimum topological view. Nevertheless, the morphology was extremely fine-structured (see also Fig. 7 below) so that it was not possible to definitely distinguish between segregated Ag and ceramic grains. Secondly, in order to obtain information about the chemical elements an analysis of polished cross-sections was carried out in "back-scattered electron (BSE) mode". Solid Ag metal could not be detected either by an element contrast in the BSE mode or by an energy dispersive X-ray analysis (EDX) analysis.

The main drawback of the Ag-containing cells sintered at 920 °C is the low current density in comparison to current densities of about 0.8 A/cm^2 (at 0.7 V, 800 °C) for Ag-free cells with cathodes that were sintered at 1,100 °C (Fig. 6) [11]. These two types of fuel cells significantly differ in the microstructure of their cathodes (Fig. 7). The cathode functional layer of the cell sintered at 920 °C exhibits very fine particles of the cathode powder in the range of about 50–100 nm and a high porosity. In principle, this microstructure should lead to a high number of electrochemically active sites and therefore to increased performance [12]. However, there are only a few small sintering necks visible between the grains and no sintering necks to the electrolyte. In contrast, the cell sintered at 1,100 °C shows a tight junction between the cathode grains and to the electrolyte layer. The reduced current densities of the fuel cells (with and without Ag) sintered at 920 °C are presumably due to this poor sintering between the cathode layer and the electrolyte (Fig. 7). The apparent activation energy of the cells with Ag-free cathodes sintered at 1,100 °C is 0.72 ± 0.075 eV, which is significantly lower than the apparent activation energy of the Ag-free samples sintered at 920 °C, but is comparable to the Ag-containing specimens. However, the pre-exponential factor is significantly smaller for the cells with cathodes sintered at 1,100 °C, which indicates that the higher sintering temperature does not only influence the apparent activation energy.

Another set of cells with cathodes containing 2 wt% Ag were sintered at 1,100 °C for 3 h, despite the low melting point of Ag. According to a chemical analysis, about 60% of the initial Ag in the doped $La_{0.65}Sr_{0.3}MnO_{3-\delta}$ cathode material evaporated during sintering. The electrochemical performance of these cells was remarkably higher than the cells sintered at 920 °C. Nevertheless, the performance was similar to cells without Ag (Table 2, right column). Obviously, the sintering step at 1,100 °C led to significantly better contact between the cathode particles and the electrolyte. Moreover, sintering of YSZ particles at temperatures as low as 920 °C might be insufficient to create a

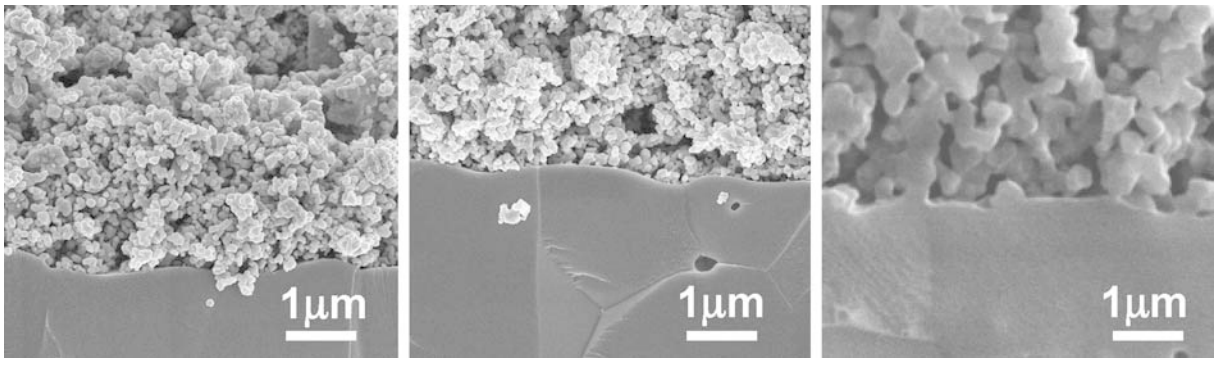

Fig. 7 Scanning electron micrographs of fracture surfaces of the cathode functional layer-electrolyte interface of a cell without Ag (*left*) and with 1 wt% Ag in the cathode (*middle*), both sintered at 920 °C, and of a Ag-free cell that was sintered at 1100 °C (*right*)

Table 2 Electrochemical performance of SOFCs sintered at 1,100°C for 3 h

Temperature (°C)	Cathodes with 2 wt% Ag: current density (A/cm^2)	Cathodes without Ag: current density (A/cm^2)
850	1.06 ± 0.06	1.12 ± 0.12
800	0.82 ± 0.03	0.81 ± 0.08
750	0.52 ± 0.01	0.52 ± 0.06
700	0.33 ± 0.01	0.32 ± 0.04

coherent YSZ network, which is necessary for a large three-phase boundary.

To conclude the SOFC cathode material $La_{0.65}Sr_{0.3}MnO_{3-\delta}$ with small amounts of very finely and homogeneously distributed Ag (0.1 to 2.0 wt% Ag) was prepared by the Pechini method. The solubility of Ag in the $La_{0.65}Sr_{0.3}MnO_{3-\delta}$ perovskite was lower than about 1 wt%. Higher amounts of Ag were segregated as solid metal.

SOFCs made with this type of cathode produced a current density of about 0.5 A/cm^2 at 800 °C and 0.7 V cell voltage. The low sintering temperature of 920 °C, which was chosen due to the low melting point of Ag, led to limited sintering of the functional layer and adhesion to the electrolyte. This poor contact is thought to be the main reason for power densities of these cells being only moderate.

Acknowledgements The authors thank the Central Department of Analytical Chemistry of Forschungszentrum Jülich for ICP-OES measurements. Thanks are also due to D. Rutenbeck for the preparation of the Ag-free samples sintered at 920 °C, P. Lersch for XRD measurements and C. Tropartz, B. Roewekamp and H. Wesemeyer for performing the electro-chemical tests. Financial support from the Federal Ministry of Research and Education, under contract no. 01SF0039, is gratefully acknowledged.

References

1. Wang S, Kato T, Nagata S, Honda T, Kaneko T, Iwashita N, Dokiya M (2002) Solid State Ionics 146 203
2. Choudhary VR, Uphade BS, Pataskar SG (1999) Fuel 78:919
3. Tikhonovich VN, Kharton VV, Naumovich EN, Savitsky AA (1998) Solid State Ionics 106:197
4. Rutenbeck D, Haanappel VAC, Mai A, Uhlenbruck S, Tietz F, Vinke IC, Stöver D (2003) Noble metals in SOFC cathodes: processing and electrochemical perfomance. In: Singhal SC, Dokiya M (eds) 8th Int Symp of Solid Oxide Fuel Cells (SOFC-VIII), vol. 2003–07. The Electrochemical Society, Pennington, N.J., USA, 2003, pp 615–623
5. Pechini MP (1967) USA Patent No. 3,330,697
6. Stochniol G, Gupta A, Naoumidis A, Stöver D (1997) $La_{0.75}Sr_{0.2}Mn_{0.9}Co_{0.1}O_3$ as cathode material for SOFC. In: Stimming U., Singhal SC, Tagawa H, Lehnert W (eds), 7th Int Symp of Solid Oxide Fuel Cells (SOFC-V), vol. 97–40. The Electrochemical Society, Pennington, N.J., USA, pp 888–896
7. Meulenberg WA, Menzler NH, Buchkremer HP, Stöver D (2002) Manufacturing routes and state-of-the-art of the planar Jülich anode supported concept for solid oxide fuel cells. In: Manthiram A, Kumta PN, Sundaram SK, Ceder G (eds), Ceram Trans: Materials for Electrochemical Energy Conversion and Storage, vol 127. The American Ceramic Society, Westerville, Ohio, USA, pp 99–108
8. Simwonis D, Naoumidis A, Dias FJ, Linke J, Moropoulou A (1997) J Mater Res 12:1508
9. Hassan AAE, Menzler NH, Blass G, Ali ME, Buchkremer HP, Stöver D (2002) Adv Eng Mater 4:125
10. de Haart LGJ, Mayer K, Stimming U, Vinke IC (1998) J Power Sources 71:302
11. Stöver D., Buchkremer HP, Tietz F, Menzler NH (2002) Trends in Processing of SOFC Components. J. Huijsmans (ed) Proc of the 5th European Solid Oxide Fuel Cell Forum, vol. 1. European Fuel Cell Forum, Lucerne, Switzerland, pp 1–9
12. Ahmad-Khanlou A, Tietz F, Vinke IC, Stöver D (2001) Electrochemical and microstructural study of SOFC cathodes based on $La_{0.65}Sr_{0.3}MnO_3$ and $Pr_{0.65}Sr_{0.3}MnO_3$. In: Yokokawa H, Singhal SC (eds), Proc 7th Int Symp of Solid Oxide Fuel Cells (SOFC-VII). The Electrochemical Society, Pennington, N.J., USA, pp 476–484